Case Studies in Chemical and Environmental Engineering 9 (2024) 100697

Contents lists available at ScienceDirect

Case Studies in Chemical and Environmental Engineering

journal homepage: www.sciencedirect.com/journal/case-studies-in-chemical-and-environmental-engineering

Case Report

Mathematical models of controlled drug release applied to an encapsulation system of food active compounds

Jesica Daiana Oroná, Susana Elizabeth Zorrilla, Juan Manuel Peralta *

Instituto de Desarrollo Tecnológico para la Industria Química (INTEC), Universidad Nacional del Litoral – CONICET, Güemes 3450, S3000GLN, Santa Fe, Argentina

ARTICLE INFO

Keywords:
Mathematical models
Transport phenomena
Encapsulation
Foods

ABSTRACT

The release of an encapsulated food active compound (model case: astaxanthin encapsulated in alginate matrix) was described by simple mathematical models from the pharmaceutical field. The models considered dissolution, diffusion, erosion, or swelling. The errors ranged from 17.6% to 49.2%. The active diffusion coefficient was in the order of 10^{-12} m^2/s. The model case required considering dissolution, erosion, and matrix changes (due to water uptake). The proposed models and determined parameters can be considered as basic tools to simplify the analysis and identification of the phenomena governing the release of food active compounds for a wide range of scenarios.

1. Introduction

The growing need of consumers for natural and healthy foods has driven the food industry to develop products enriched with active compounds (*e.g.*, phenolic compounds and vitamins). These compounds are obtained from natural sources and have potential benefits for health, such as antioxidant, anti-inflammatory, and antimicrobial properties. However, certain compounds are sensitive to environmental factors such as pH, light, oxygen, temperature, and enzymatic degradation [1], which limits their direct incorporation into foods. These and other limitations can be overcome by encapsulation to protect the active compounds, control their release, mask off-flavor, or reduce the degradation in the gastrointestinal tract [2].

In general, encapsulation systems of food active compounds are designed not only to protect the active ingredient but also to ensure its release at a desired site for a given period [3]. In this regard, the mathematical modeling can be an essential tool to predict and analyze the release of active compounds, study the influence of formulation and other factors on the release mechanisms, and to reduce the number of experiments [3,4].

In the literature, a limited number of mathematical models to describe the release of food active compounds are available [5,6]. Nevertheless, some models developed to predict controlled drug release have been successfully used in food systems [3,7]. This connection can be explained by the similarities of targeted/controlled release of pharmaceutical and food products designed to deliver an encapsulated ingredient in the gastrointestinal tract [8].

Release modeling can be based on empirical, semi-empirical or mechanistic approaches. The main advantage of mechanistic models is their fundamental basis that allows representing different mechanisms (*e.g.*, diffusion, erosion, swelling, dissolution, etc.) and extending the results to hypothetical scenarios [8]. Among the mechanistic models used to predict controlled drug release, those that combine two mechanisms can be a simple approach to analyze the release profiles from food delivery systems. The objective of this work was to predict the release of an encapsulated food active compound (active) using simple mathematical models developed in the pharmaceutical field that combine two mechanisms. In this way, the progress achieved in the pharmaceutical field can be applied in the food area as an intermediate degree of complexity between the processes described by a single mechanism (in general, diffusion) and those that consider numerous phenomena whose solution is more complex.

2. Materials and methods

The release of astaxanthin from an alginate matrix particle was chosen as a model system of food active release. The description of the basic phenomena was tested with simple mechanistic mathematical models of controlled drug release found in the literature. Each model simultaneously describes a specific pair of phenomena generally involved in the process, representing the active diffusion and matrix erosion [9], the active diffusion and dissolution [10], and the active diffusion and matrix swelling [11].

* Corresponding author.
E-mail address: jmperalta@intec.unl.edu.ar (J.M. Peralta).

https://doi.org/10.1016/j.cscee.2024.100697
Received 7 September 2023; Received in revised form 22 February 2024; Accepted 18 March 2024
Available online 27 March 2024

Nomenclature

Bi	mass Biot number [−]
c_A	active concentration [mol/m^3]
$c_{A,0}$	initial active concentration [mol/m^3]
c_s	active saturation concentration in the system [mol/m^3]
c_w	water concentration [mol/m^3]
c_w^*	critical water concentration [mol/m^3]
c_w^{eq}	water concentration in the equilibrium [mol/m^3]
$c_{w,0}$	initial water concentration [mol/m^3]
D_0	initial active diffusion coefficient [m^2/s]
D_A	active diffusion coefficient [m^2/s]
$D_{A,m}$	active diffusion coefficient in the matrix [m^2/s]
$D_{A,w}$	active diffusion coefficient in water [m^2/s]
D_t	diffusion coefficient of active at time t [m^2/s]
D_w	self-diffusion coefficient of water [m^2/s]
$D_{w,0}$	active diffusion coefficient at time t [m^2/s]
$D_{w,m}$	total water diffusion coefficient [m^2/s]
$D_{w,m}^f$	water diffusion coefficient in the matrix associated with the Fickian flux [m^2/s]
$D_{w,m}^r$	water diffusion coefficient in the matrix associated with the non-Fickian flux [m^2/s]
$D_{w,s}$	water diffusion coefficient in the dry matrix [m^2/s]
De	Deborah number [−]
Di	dissolution/diffusion number [−]
F_E	factor considering the erosion contribution on the release process [−]
h	superficial transfer coefficient of dissolved active [m^2/s]
J	number of experimental data [−]
k	a first-order dissolution constant that characterizes the dissolution rate of the active in the absence of the matrix [1/s]
k_e	coefficient that describes the probability of branching of activated sites in the time interval from oligomer generation to its dissolution [1/s]
k_s	parameter for the cleavage rate of the polymeric chain [1/s]
$MAPE$	mean absolute percentage error [%]
n	n-th term of the infinite sum [−]
N	number of experimental data [−]
p_v	probability of the local volume expansion [−]
p_w	probability factor of water absorption [−]
r	radial position [m]
R	sphere radius [m]
R_0	initial system radius [m]
R_d	parameter related to the non-Fickian nature of the water uptake [−]
R_g	radius of the glassy matrix region [m]
R_t	system radius at time t [m]
Sh	Sherwood number [−]
t	time [s]
T_m	time of maximum erosion rate of the matrix [s]
V_0	initial volume of the system [m^3]
v_∞	velocity of surrounding medium [m/s]
V_t	system volume at time t [m^3]

Greek symbols

α_n	n-th root of $\alpha_n R\cot(\alpha_n R) + Bi = 1$ [1/m]
β_1	constant [m^3/mol]
β_2	constant [m^3/mol]
β_3	constants [m^3/mol]
ε	system porosity [−]
λ^{eq}	relaxation constant for the swelling matrix in the equilibrium [s]
ρ_w	water density [mol/m^3]
τ	Fourier number [−]
Φ_L	volume-averaged fraction of released active [−]
$\Phi_{LE,i}$	i-th value of experimental Φ_L [−]
$\Phi_{LT,i}$	i-th value of theoretical Φ_L [−]
Φ_w	the volume-averaged fraction of absorbed water [−]

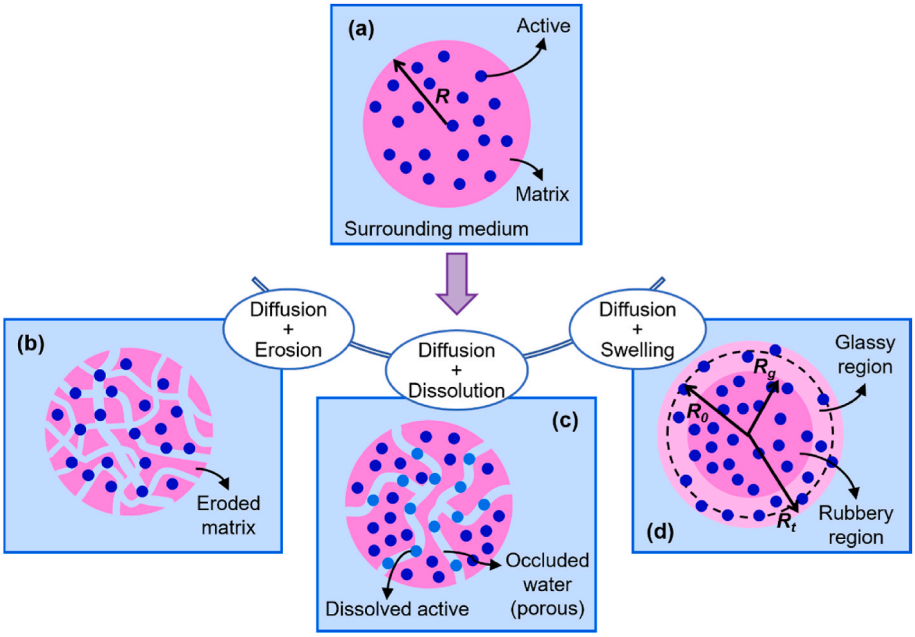

Fig. 1. **(a)** Physical system schematics and mechanisms considered by **(b)** He et al. [9], **(c)** Harland et al. [10], and **(d)** Wu and Brazel [11].

2.1. Diffusion and erosion

2.1.1. Physical model

The physical model is assumed to be a spherical particle of radius R composed of an active and a polymeric matrix surrounded by liquid (Fig. 1a). Here, the active can diffuse through the entire system (matrix and liquid) and the polymeric chain of the matrix can be cleaved (*i.e.,* erosion) (Fig. 1b).

2.1.2. Mathematical model

He et al. [9] proposed a mathematical model for the system described in Fig. 1a. The model considers that the release kinetics of an active from a bioerodible polymeric matrix can be described by a combination of the active diffusion and the matrix erosion. These authors considered that (a) initially the active is dispersed in the matrix, (b) the matrix erosion is completed at the end of the release process, and (c) the phenomena occur mainly in the radial direction r. Accordingly, the mathematical model (analytical solution) is,

$$\Phi_L = 6\sqrt{\frac{D_t t}{\pi R^2}} - 3\frac{D_t}{R^2} + F_E\left[\frac{\exp(k_e t - k_e T_m)}{1+\exp(k_e t - k_e T_m)}\right] \tag{1}$$

where Φ_L is the fraction of released active at time t [−], D_t is the active diffusion coefficient at time t [m^2/s], F_E is a factor considering the erosion contribution to the release process [−], k_e is a coefficient that describes the probability of branching of activated sites in the time interval from oligomer generation to its dissolution [1/s], and T_m is the time of maximum erosion rate of the matrix [s]. The factor F_E indicates that a fraction of the active originally released to dissolution medium by diffusion now releases due to the matrix erosion. The time T_m is a descriptive value of the half erosion time and it is related to the polymer chain scission rate.

The first two terms of **Eq. (1)** take into account the contribution of the active diffusion to the release process and the erosion effect on the active diffusion. These terms are the result of solving the Fick equation for a sphere, considering a constant concentration of the active at the surface, a constant diffusion coefficient, and a short-time limit ($\Phi_L \leq 0.6$). The erosion effect on the active diffusion was included through a variable diffusion coefficient due to cleavage of the polymeric chain of the matrix (D_t),

$$D_t = D_0 \exp(k_s t) \tag{2}$$

where D_0 is the initial active diffusion coefficient [m^2/s] and k_s is a parameter for the cleavage rate of the polymeric chain [1/s] described by an autocatalyzed first-order reaction. This parameter is directly related to the reactivity of the bonds within the polymeric chain.

The third term of **Eq. (1)** takes into account the erosion contribution to the active release. This term describes the matrix erosion as a combined process of the branching and termination of polymer decomposition caused by the formation of activated nuclei in the matrix, which formed on the system surface and spread inwards. The matrix degradation starts in those nuclei generating oligomers of different molecular weights and increasing the system porosity [12].

2.2. Diffusion and dissolution

2.2.1. Physical model

The physical model is similar to the previous case assuming a spherical particle of radius R composed of an active and a polymeric matrix surrounded by liquid (Fig. 1a). Here, the active is initially non-dissolved in the matrix but once the particle is placed in the aqueous surrounding medium, the active starts dissolving and then it diffuses through the matrix pores to the surrounding liquid (Fig. 1c).

2.2.2. Mathematical model

The system presented in Fig. 1a can be described by the mathematical model proposed by Harland et al. [10]. This model is based on solving a mass balance for the active considering two boundary conditions at the surface and that the release process of the active depends on the dissolution of the non-dissolved active coupled to the diffusion of dissolved active (Fig. 1c). The authors considered that (a) the phenomena mainly occur in the radial direction r, (b) the initial active concentration ($c_{A,0}$) is higher than its solubility in the system (εc_s), and (c) the matrix is non-swellable and non-erodible. On that basis, the mass balance for the active is ($0 \leq r < R$, $t > 0$),

$$\frac{\partial c_A}{\partial t} = D_A\left(\frac{\partial^2 c_A}{\partial r^2} + \frac{2}{r}\frac{\partial c_A}{\partial r}\right) + k(\varepsilon c_s - c_A) \tag{3}$$

where c_A is the active concentration [mol/m^3], D_A is the active diffusion coefficient [m^2/s], k is a first-order dissolution constant that characterizes the dissolution rate of the active in the absence of the matrix [1/s], ε is the system porosity [−], and c_s is the active saturation concentration in the system [mol/m^3].

The first term of **Eq. (3)** describes the active diffusion in the pores formed in the matrix due to the continuous active dissolution. This mechanism is characterized by a constant diffusion coefficient of the active. The second term describes the active dissolution. This term will be negligible if the initial active concentration is lower than its solubility in the system ($c_{A,0} \leq \varepsilon c_s$), and **Eq. (3)** is reduced to the classic Fickian diffusion equation.

Equation (3) was solved using the initial condition given by **Eq. (4)**, a symmetry condition at the center of the system (**Eq. (5)**) and a perfect sink condition (*PSC*, **Eq. (6)**) and a finite external convective resistance condition (*FRC*, **Eq. (7)**) at the surface of the system.

Initial condition (PSC and FRC):

$$c_A = c_{A,0}, \quad 0 \leq r \leq R, \quad t = 0 \tag{4}$$

Symmetry condition (PSC and FRC):

$$\frac{\partial c_A}{\partial r} = 0, \quad r = 0, \quad t > 0 \tag{5}$$

Perfect sink condition (PSC):

$$c_A = 0, \quad r = R, \quad t > 0 \tag{6}$$

Finite external convective resistance condition (FRC):

$$-D_A\frac{\partial c_A}{\partial r} = h(c_s - c_A), \quad r = R, \quad t > 0 \tag{7}$$

The analytical solution of **Eq. (3)** using *PSC* is,

$$\Phi_L = 6\sum_{n=1}^{\infty}\frac{(Di + n^2\pi^2)Di\,\tau + n^2\pi^2\{1-\exp[-(Di+n^2\pi^2)\tau]\}}{(Di+n^2\pi^2)^2} \tag{8}$$

The analytical solution of **Eq. (3)** using *FRC* is,

$$\Phi_L = 6Bi^2\sum_{n=1}^{\infty}\frac{\left(Di+\alpha_n^2R^2\right)Di\tau + \alpha_n^2R^2\left\{1-\exp\left[-\left(Di+\alpha_n^2R^2\right)\tau\right]\right\}}{\left(Di+\alpha_n^2R^2\right)^2\left[\alpha_n^2R^2 + Bi(Bi-1)\right]} \tag{9}$$

where Di is the dissolution/diffusion number (kR^2/D_A) [−], τ is the Fourier number ($D_A t/R^2$) [−], Bi is the mass Biot number [−] and α_n is the n-th root of $\alpha_n R\cot(\alpha_n R) + Bi = 1$ [1/m]. Here, Di represents the relative importance of the dissolution and diffusion phenomena on the overall release process. The authors assumed that the active diffusion coefficients in the matrix and in the surrounding liquid have the same order of magnitude. Then, $Bi \approx hR/D_A$.

2.3. Diffusion and swelling

2.3.1. Physical model

Again, the physical model is similar to the previous cases assuming a spherical particle of initial radius R_0 composed of an active and a polymeric glassy matrix surrounded by liquid (Fig. 1a). Here, the

external liquid (water) can diffuse into the particle. As water enters the particle, its concentration (c_w) increases until it reaches a critical value (c_w^*) where the matrix is relaxed and changes its state from glassy to rubbery (swelling). Therefore, as time progresses, the active can diffuse to the surrounding liquid, the particle radius (R_t) increases, and the radius of the glassy matrix region (R_g) decreases (Fig. 1d).

2.3.2. Mathematical model

Wu and Brazel [11] proposed a model for a system similar to the one presented in Fig. 1a and solved it for a disc-shaped particle. In the present work, this model was solved for a spherical particle.

The main assumptions of this model are: (a) the polymer relaxation is much slower than the water diffusion in the glassy region ($c_w < c_w^*$), *i.e.*, both the polymer relaxation and volume expansion are negligible in this region, (b) perfect mixing in the rubbery region ($c_w \geq c_w^*$), (c) the active volume is negligible, and (d) the main phenomena occur in the radial direction r. Therefore, the mass balances of water and active are,

Water ($0 \leq r < R_t$, $t > 0$):

$$\frac{\rho_w}{(\rho_w - c_w)}\frac{\partial c_w}{\partial t} = \frac{1}{r^2}\frac{\partial}{\partial r}\left(r^2 D_{w,m}^f \frac{\partial c_w}{\partial r}\right) + \frac{p_w}{r^2}\frac{\partial}{\partial r}\left(r^2 D_{w,m}^r \frac{\partial c_w}{\partial r}\right) \tag{10}$$

Active ($0 \leq r < R_t$, $t > 0$):

$$\frac{\partial c_A}{\partial t} = \frac{1}{r^2}\frac{\partial}{\partial r}\left(r^2 D_{A,m}\frac{\partial c_A}{\partial r}\right) - p_v \frac{c_A}{(\rho_w - c_w)}\frac{\partial c_w}{\partial t} \tag{11}$$

where R_t is the system radius at time t [m], ρ_w is the water density [mol/m^3], $D_{w,m}^f$ is the water diffusion coefficient in the matrix associated with the Fickian flux [m^2/s], $D_{w,m}^r$ is the water diffusion coefficient in the matrix associated with the non-Fickian flux [m^2/s], p_w is a probability factor of water absorption accounting how fast the polymer chains are relaxed to accommodate the water accumulation [−], $D_{A,m}$ is the active diffusion coefficient in the matrix [m^2/s], and p_v is the probability of the local volume expansion [−].

The parameters of Eqs. (10) and (11) can be calculated as,

$$D_{w,m}^f = D_{w,s} \tag{12}$$

$$D_{w,m}^r = \left\{D_w \exp\left[-\beta_1\left(c_w^{eq} - c_w\right)\right] - D_{w,m}^f\right\} H\left(c_w - c_w^*\right) \tag{13}$$

$$D_{A,m} = \left\{D_{A,w} \exp\left[-\beta_3\left(c_w^{eq} - c_w\right)\right]\right\} H\left(c_w - c_w^*\right) \tag{14}$$

$$p_w = \exp\left\{\left\{1 - \exp\left[\beta_2\left(c_w^{eq} - c_w\right)\right]\right\}\lambda^{eq}\frac{V_0^2}{V_t^2}\frac{D_{w,m}}{R_0^2}\right\} \tag{15}$$

$$p_v = H\left(c_w - c_w^*\right) \tag{16}$$

where $D_{w,s}$ is the water diffusion coefficient in the dry matrix [m^2/s], D_w is the self-diffusion coefficient of water [m^2/s], c_w^{eq} is the water concentration in the equilibrium [mol/m^3], $D_{A,w}$ is the active diffusion coefficient in water [m^2/s], $D_{w,m}$ is the total water diffusion coefficient ($D_{w,m} = D_{w,m}^f + D_{w,m}^r$) [m^2/s], λ^{eq} is a relaxation constant for the swelling matrix in the equilibrium [s], V_0 and V_t are the initial volume and the system volume at time t [m^3], respectively, β_1, β_2 and β_3 are constants [m^3/mol], and $H(x)$ is a Heavyside step function that is 1 if $x \geq 0$ and is 0 if $x < 0$.

The model considers that the evolution of the system radius R_t can be estimated assuming that the volume expansion occurs only in the rubbery region and that the active volume is negligible. Therefore, the expression for R_t is,

$$R_t = R_0\left\{1 + \frac{3}{R_0^3}\int_{R_g}^{R_t} r^2\frac{c_w}{\rho_w}dr - \frac{c_w^*}{\rho_w}\left[1 - \left(\frac{R_g}{R_0}\right)^3\right]\right\}^{1/3} \tag{17}$$

The system of Eqs. (10) and (11) were solved using the initial and boundary conditions given by Eqs. (18)–(22).

Initial conditions:

$$c_w = c_{w,0}, \quad 0 \leq r \leq R_0, \quad t = 0 \tag{18}$$

$$c_A = c_{A,0}, \quad 0 \leq r \leq R_0, \quad t = 0 \tag{19}$$

Boundary conditions:

$$\frac{\partial c_w}{\partial r} = \frac{\partial c_A}{\partial r} = 0, \quad r = 0, \quad t > 0 \tag{20}$$

$$c_w = c_w^{eq}, \quad r = R_t, \quad t > 0 \tag{21}$$

$$c_A = 0, \quad r = R_t, \quad t > 0 \tag{22}$$

Taking into account the volume variation of the particle (Eq. (17)), the profiles of the volume-averaged fraction of the absorbed water (Φ_w) [−] and the volume-averaged fraction of the released active (Φ_L) [−] were calculated based on the local profiles of c_w and c_A, respectively,

$$\Phi_w = \frac{1}{V_t}\int_{V_t}\left(\frac{c_w}{c_w^{eq}}\right)dV \tag{23}$$

$$\Phi_L = 1 - \frac{1}{V_t}\int_{V_t}\left(\frac{c_A}{c_{A,0}}\right)dV \tag{24}$$

2.4. Experimental data and numerical resolution

The experimental data of the *in vitro* release of astaxanthin from spherical particles of calcium alginate, presented by Niizawa et al. [13], were used to fit the mathematical models presented in Sections 2.1. to 2.3. The active release profiles were obtained in simulated intestinal conditions using a 0.05 M phosphate buffer (pH 7.4) as the dissolution media at 37 °C and 100 rpm of agitation.

The mathematical models were fitted to the experimental data using the *nonlin_curvefit* function (GNU/Octave 6.2.0 optimization package). The goodness of fit was evaluated through the mean absolute percentage error (*MAPE*),

$$MAPE = \frac{100}{N}\sum_{i=1}^{N}\left|1 - \frac{\Phi_{LT,i}}{\Phi_{LE,i}}\right| \tag{25}$$

where N is the number of experimental data [−], and $\Phi_{LT,i}$ and $\Phi_{LE,i}$ are the theoretical and experimental i-th values of Φ_L, respectively.

2.4.1. Known and fitted parameters

The parameters for the 3 models were separated in 2 sets: known and fitted (Table 1). The first set of parameters are R, R_0, ρ_w, $c_{A,0}$, $c_{w,0}$, c_w^{eq}, and D_w. The values of those parameters were obtained from De'Nobili et al. [14], Chiarappa et al. [5], and Oroná et al. [6]. The fitted parameters were found by initialization with values from the literature for similar systems. The values of coefficients D_A and D_0 were obtained from the literature [15]. The values of k_s, F_E, and k_e were assumed according to the ranges reported by He et al. [9] for a wide range of encapsulation systems. The value of T_{max} was assumed to be in the order of magnitude of the simulation time. The value of k was assumed to be in the order of magnitude reported by Harland et al. [10]. The initial value of h was estimated through correlations for a single sphere [16]. The initial values of λ^{eq}, c_w^*, β_1, β_2, β_3, $D_{A,w}$, and $D_{w,s}$ were assumed based on values reported by Wu and Brazel [11] for a drug-matrix system of proxyphylline-poly(vinyl) alcohol.

2.4.2. Numerical solution

The fitting procedure and simulations for the models that take into account diffusion-erosion and diffusion-dissolution were carried out

Table 1
Known values of the system parameters and initial values of the fitted parameters.

Parameter	Units	Value	Source
Known values of the system parameters			
R, R_0	m	1.02×10^{-3}	[6]
ρ_w	mol/m^3	5.56×10^{4}	[5]
$c_{A,0}$	mol/m^3	4.93	[6]
$c_{w,0}$	mol/m^3	1.00×10^{4}	[6]
c_w^{eq}	mol/m^3	5.48×10^{4}	[5]
D_w	m^2/s	2.90×10^{-9}	[14]
Initial values of the fitted parameters			
Diffusion-erosion model			
D_0	m^2/s	2.03×10^{-10}	[15]
k_s	1/s	1.00×10^{-7}	Assumed
F_E	–	0.50	Assumed
k_e	1/s	1.00×10^{-6}	Assumed
T_{max}	s	15000	Assumed
Diffusion-dissolution model			
D_A	m^2/s	2.03×10^{-10}	[15]
k	1/s	1.00×10^{-3}	Assumed
h	m/s	7.20×10^{-6}	Estimated
Diffusion-swelling model			
λ^{eq}	s	264	Assumed
c_w^*	mol/m^3	0.30 c_w^{eq}	Assumed
β_1	m^3/mol	5.40×10^{-5}	Assumed
β_2	m^3/mol	3.60×10^{-5}	Assumed
β_3	m^3/mol	1.60×10^{-4}	Assumed
$D_{A,w}$	m^2/s	8.33×10^{-10}	Assumed
$D_{w,s}$	m^2/s	0.001 D_w	Assumed

using a PC Intel Core i5 7200 of 2.70 GHz with 8 GB of RAM. Each run took approximately 0.5 s to converge. The third model (diffusion-swelling) was discretized through an explicit method. The particle radius was divided into 200 segments and the initial time step was set to 6×10^{-4} s. The step size of the spatial discretization was considered variable due to the volume variation of the particle. The simulations were carried out using the Pirayu cluster [17]. Each simulation took approximately 72 h to converge.

3. Results and discussion

3.1. Diffusion-erosion model

The fitted values of the model parameters found for the astaxanthin/calcium alginate encapsulation system are shown in Table 2. The *MAPE* value obtained was 35.8%, which means that the fit was reasonable [18].

Table 2
Fitted values of the parameters for the models.

Parameter	Units	Value	*MAPE*
Diffusion-erosion model			
D_0	m^2/s	4.57×10^{-12}	35.8%
k_s	1/s	9.59×10^{-5}	
F_E	–	0	
k_e	1/s	0	
T_{max}	s	22758	
Diffusion-dissolution model			
Perfect sink condition (PSC)			
D_A	m^2/s	6.00×10^{-12}	38.7%
k	1/s	5.78×10^{-5}	
Finite external convective resistance condition (FRC)			
D_A	m^2/s	8.51×10^{-12}	17.6%
k	1/s	4.74×10^{-6}	
h	m/s	8.33×10^{-6}	
Diffusion-swelling model			
λ^{eq}	s	1314	49.2%
c_w^*	mol/m^3	0.9 c_w^{eq}	
β_1	m^3/mol	6.84×10^{-5}	
β_2	m^3/mol	2.68×10^{-4}	
β_3	m^3/mol	4.14×10^{-5}	
$D_{A,w}$	m^2/s	9.27×10^{-12}	
$D_{w,s}$	m^2/s	0.001 D_w	

Although there are no measurements of diffusion coefficient of astaxanthin (in soybean oil to form an oleoresin) in calcium alginate, some experimental values from literature for similar systems can be used to validate the fitted value of D_0 presented in Table 2. The same rationale will be used when needed for the rest of the fitted parameters. The fitted value of D_0 was in the order of magnitude of the diffusion coefficient of molecules in polymers [19]. Colín-Chávez et al. [20] evaluated the diffusion coefficient of astaxanthin diffusing from a monolayer low-density polyethylene film and a two-layer high-density polyethylene/low-density polyethylene film to a fatty food simulant (95% ethanol solution). These authors found that the diffusion coefficient of astaxanthin was 7.40 ($\pm$0.00) $\times$ 10^{-15} m^2/s and 5.59 ($\pm$0.07) $\times$ 10^{-15} m^2/s in the monolayer and in the two-layer films, respectively, at 30 °C. Karki et al. [15] estimated by molecular dynamic simulations values of the diffusion coefficient for astaxanthin in water and ethanol of 2.03 ($\pm$0.01) $\times$ 10^{-10} m^2/s and 1.8 ($\pm$0.3) $\times$ 10^{-10} m^2/s at 27 °C, respectively. Thus, the fitted value of D_0 found in this work was considered acceptable.

The fitted values of F_E and k_e were zero (Table 2). As described in Section 2.1.2, the third term is related to the branching and termination of polymer decomposition on the system surface that spread inwards. This would mean that, for the system studied in this work, the erosion of the matrix from the surface would be negligible [9]. However, it was found that the erosion due to cleavage of the polymeric chain of the matrix was not negligible since the fitted value of k_s was 9.59×10^{-5} 1/s (Table 2). This feature can be correlated with what several authors reported for calcium alginate gels in intestinal conditions that become increasingly porous and weak until disintegration [21].

Fig. 2 shows the comparison between the experimental data and the theoretical profile for Φ_L (using the parameters of Table 2) as a function of $t^{1/2}$. The theoretical profile shows the level of agreement that was reported by the *MAPE* value. However, the degree of description was greatly reduced at the beginning ($t^{1/2} < 30$ s$^{1/2}$) of the experiment. This could be due to the fact that the model, at short times, considers a predominantly Fickian release [9] as confirmed by the overlapping with the profile for a purely diffusive release ($k_s = 0$ and $F_E = 0$). Fig. 2 also shows that when the erosion phenomenon is neglected, lower Φ_L values are obtained resulting in a considerably reduced amount of release at the end of the experiment ($t^{1/2} = 120$ s$^{1/2}$).

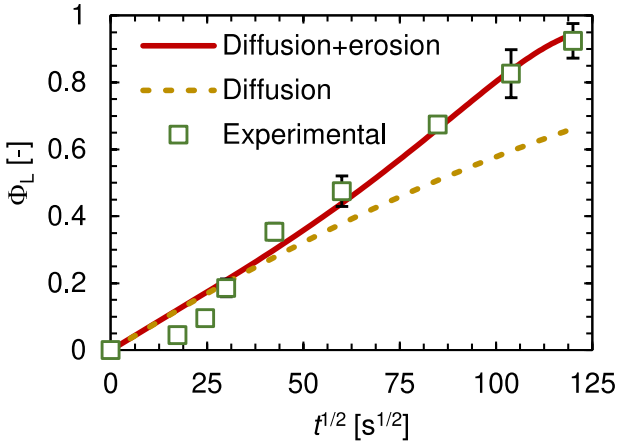

Fig. 2. Comparison between the experimental data (squares) and the theoretical profiles of the diffusion + erosion model (solid line) for Φ_L as a function of $t^{1/2}$. Dashed line corresponds to a purely diffusive system ($k_s = 0$). Error bars represent the standard deviation of 5 independent replicates.

3.2. Diffusion-dissolution model

Table 2 shows the fitted parameters values of the mathematical model. The *MAPE* values were 38.7% and 17.6% for the model with *PSC* and *FRC*, respectively. The goodness of fit was considered reasonable for the first case and good for the second case [18].

Here, the fitted values of D_A for both conditions are of the same order of magnitude as the fitted value of D_0 obtained in Section 3.1 (Table 2). The value of k for *PSC* is an order of magnitude greater than the value of k for *FRC*. This would mean that the active dissolves faster in the first case [22]. The values of k are expected to be small due to the poor solubility of astaxanthin in water [23]. In this regard, Yan et al. [24] informed a $k = \mathcal{O}(10^{-6})$ 1/s for a compound poorly soluble in water. The fitted value for h was similar to the estimated value (Table 1) which was obtained from correlations for single spheres [16] considering a diffusion coefficient equal to the fitted D_A for *FRC* (Table 2).

The comparison between experimental data and theoretical profiles for Φ_L (using the parameters of Table 2) is shown in Fig. 3. Here, the Φ_L profile obtained for *FRC* fitted better to experimental data than the one for *PSC*. This could be due to the fact that the model for *PSC* predicts a negligible external resistance to diffusion (*i.e.,* perfect mix or $h \to \infty$). This condition is not expected for astaxanthin diffusing from calcium alginate matrix into the aqueous medium under gastrointestinal conditions. This can be estimated using the correlation [16]: $h \approx 0.8 v_\infty^{1/3} (D_A/R)^{2/3}$. Here, the maximum value in the gastrointestinal tract is $v_\infty \approx 0.04$ m/s [25], and $D_A/R = \mathcal{O}(10^{-8})$ (Tables 1 and 2). So, $h = \mathcal{O}(10^{-6})$ which is a very different value than the one assumed for *PSC*.

Although the diffusion-dissolution model with *FRC* assumed a constant active diffusion coefficient and a non-swellable and non-erodible matrix (**Section 2.2**), a reasonable goodness of fit to the experimental data was obtained. As implied in **Section 3.1**, several authors reported that calcium alginate gels undergo swelling and erosion in intestinal conditions [21]. Based on this idea, Wu and Brazel [11] used a variable diffusion coefficient for modeling the active transport in swellable matrices, which depends on the local water concentration. Also, Oroná et al. [6] reported that, in the astaxanthin-calcium alginate system, the release of the active was strongly affected by the erosion and the modifications in the matrix structure. Consequently, the goodness of fit obtained for the model with *FRC* could be explained by considering the parameter h as an effective parameter that could partially include the other effects (*e.g.*, erosion and swelling) observed in the experimental system.

3.3. Diffusion-swelling model

Table 2 shows the fitted values of the model parameters obtained for the system astaxanthin/calcium alginate. The value of *MAPE* was 49.2%, which made the fit inaccurate [18].

The fitted relaxation time (λ^{eq}) was 1314 s, which is higher than the values reported in the literature for systems containing calcium alginate. Ahearne et al. [26] reported values in the order of 200 s. This discrepancy could be attributed to the structural differences between the alginate samples since the ratios and lengths of the G and M blocks affect considerably their mechanical behavior [26]. The effect of λ^{eq} on the release can be analyzed through the Deborah number (*De*) and a parameter related to the non-Fickian nature of the water uptake (R_d) [27],

$$De = \frac{\lambda^{eq}}{R_t^2/D_w} \tag{26}$$

$$R_d = \frac{D_w}{D_{w,m}^f} \tag{27}$$

Here, *De* is defined as the ratio of the characteristic times of the matrix relaxation to the water diffusion. If $De \ll 1$, the matrix relaxation is produced instantly. Conversely, if $De \gg 1$, the matrix relaxation occurs in a very long time. A value of $De \approx 1$ means that the relaxation and water diffusion phenomena occur in the same time scale, and non-Fickian phenomena are expected to govern the water uptake [28]. Similar information can be extracted from **Eq. (27)**. A value of $R_d = 1$ means that the water flux follows a Fick's kinetics. The further R_d deviates from 1, the more non-Fickian is the flux. In this study, the values of these parameters were $De \approx 3.7$ and $R_d \approx 1000$. This suggests that the water uptake is governed by a non-Fickian kinetics, which is consistent with literature regarding water sorption and diffusion in alginate-based hydrogels [29]. The values of R_d and *De* were calculated using the $D_w = 2.9 \times 10^{-9}$ m^2/s [30], the fitted values of the parameters $D_{w,m}$ and λ^{eq} (Table 2), and $R_t = R_0$ (Table 1).

Table 2 shows that the fitted values of the parameters β_1, β_2, and β_3 were in the range of 4.14×10^{-5} to 2.68×10^{-4} m^3/mol. These values are in agreement with those reported in the literature for similar systems (3.6×10^{-4} m^3/mol to 1.6×10^{-4} m^3/mol [11]). The value of $D_{A,m}$ was of the same order of magnitude that the ones found in Sections 3.1 and 3.2.

Fig. 4a shows the comparison between the experimental data and the theoretical profile for Φ_L (using the parameters of Table 2) as a function of $t^{1/2}$. Here, it is evident that the model described reasonably well only the central portion of the release, showing a poor performance at the beginning ($t^{1/2} < 35$ s$^{1/2}$) and end ($t^{1/2} > 75$ s$^{1/2}$). This behavior could be partially explained analyzing the profiles for Φ_w and R_t/R_0 (Fig. 4b). Firstly, the system quickly reaches a rubbery state at $t^{1/2} \approx 35$ s$^{1/2}$ when $\Phi_w \geq \Phi_w^*$ (*i.e.*, $c_w = c_w^*$). Then, Φ_w tends asymptotically to 1. This means that $c_w \to c_w^{eq}$ throughout the system volume. Secondly, three stages are observed in the R_t/R_0 profile. It starts with a slow increase up to $t^{1/2} = 75$ s$^{1/2}$, then continues with a stepper increase within the range of 75 s$^{1/2} \leq t^{1/2} \leq 100$ s$^{1/2}$ and, ends with a change in the slope to a concave profile for $t^{1/2} > 100$ s$^{1/2}$. Consequently, the profile fails to predict the swelling evolution of calcium alginate particles [6] and gels [21] in intestinal conditions. This could be due that the diffused water is only used in the model to increase the particle volume and does not interact with the matrix (*i.e.*, erosion) or the active (*i.e.*, dissolution).

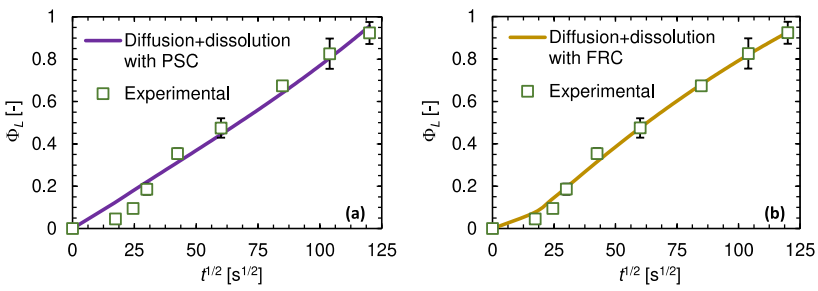

Fig. 3. Comparison between the experimental data (squares) and the theoretical profiles of the diffusion + dissolution model (solid line) for Φ_L as a function of $t^{1/2}$ with **(a)** *PSC* and **(b)** *FRC*. Error bars represent the standard deviation of 5 independent replicates.

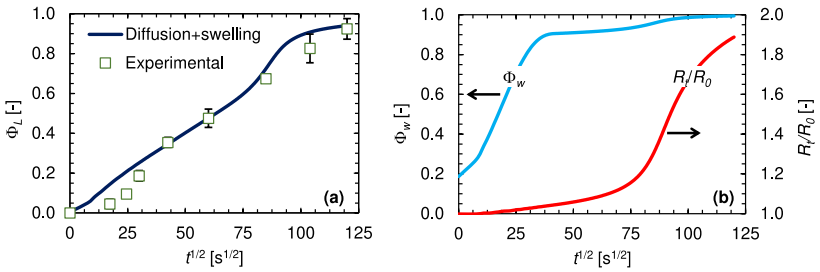

Fig. 4. **(a)** Comparison between the experimental data (squares) and the theoretical profiles of the diffusion + swelling model (solid line) for Φ_L as a function of $t^{1/2}$ and **(b)** theoretical profiles for Φ_w and R_t/R_0 as a function of $t^{1/2}$. Error bars represent the standard deviation of 5 independent replicates.

4. Conclusions

Simple mathematical models developed for the pharmaceutical field were used to predict the release of an encapsulated food active. These models combine two mechanisms generally found in the release process. The model that considered the active diffusion and matrix erosion allowed obtaining a reasonable fit (*MAPE* of 35.8%) and interpreting possible behaviors according to the parameters determined. The model that considered the active diffusion and dissolution allowed obtaining reasonable (*MAPE* of 38.7% for a perfect sink condition) and good fits (*MAPE* of 17.6% for a finite external convective resistance). In this case, it is interesting to mention that simple models can include various phenomena in effective parameters. The model that considered the active diffusion and matrix swelling fitted inaccurately the experimental data (*MAPE* of 49.2%). Although some of the parameters were in agreement with values found in the literature, the model fails to predict the swelling evolution of the particles.

Simple models developed for the pharmaceutical field may help to understand the phenomena involved in the release of food active compounds. Although reasonable fits were mostly obtained, it should be noted that a wide range of possible scenarios were covered. We believe that the included discussions may encourage the reader to represent the food active release using this approach.

Funding

This study was partially supported by Universidad Nacional del Litoral (Santa Fe, Argentina) [grant number CAI+D 506 201901 00005 LI], Agencia Nacional de Promoción de la Investigación, el Desarrollo Tecnológico y la Innovación (Agencia I+D+i) (Argentina) [grant number PICT 2020-544], and Consejo Nacional de Investigaciones Científicas y Técnicas (CONICET) (Argentina) [grant number 11220200100440CO].

CRediT authorship contribution statement

Jesica Daiana Oroná: Writing – original draft, Visualization, Validation, Software, Methodology, Investigation, Formal analysis, Data curation, Conceptualization. **Susana Elizabeth Zorrilla:** Writing – review & editing, Supervision, Resources, Project administration, Methodology, Investigation, Funding acquisition, Conceptualization. **Juan Manuel Peralta:** Writing – review & editing, Visualization, Supervision, Resources, Project administration, Methodology, Investigation, Funding acquisition, Conceptualization.

Declaration of competing interest

The authors declare that they have no known competing financial interests or personal relationships that could have appeared to influence the work reported in this paper.

Data availability

Data will be made available on request.

Acknowledgments

The authors would like to thank the UNL (Santa Fe, Argentina) [grant number CAI+D 506 201901 00005 LI], Agencia I+D+i (Argentina) [grant number PICT 2020-544], and CONICET (Argentina) (Argentina) [grant number 11220200100440CO]. The present work used computational resources of the Pirayu Cluster, acquired with funds of Agencia Santafesina de Ciencia, Tecnología e Innovación (ASACTEI), Gobierno de la Provincia de Santa Fe, through project AC-00010-18, Resolution No. 117/14. This equipment is part of Sistema Nacional de Computación de Alto Desempeño del Ministerio de Ciencia y Tecnología de la República Argentina.

References

[1] P.D. de F. Santos, F.T.V. Rubio, M.P. da Silva, L.S. Pinho, C.S. Favaro-Trindade, Microencapsulation of carotenoid-rich materials: a review, Food Res. Int. 147 (2021) 110571, https://doi.org/10.1016/j.foodres.2021.110571.

[2] K.G.D. Kaushalya, K.D.P.P. Gunathilake, Encapsulation of phlorotannins from edible brown seaweed in chitosan: effect of fortification on bioactivity and stability in functional foods, Food Chem. 377 (2022) 132012, https://doi.org/10.1016/j.foodchem.2021.132012.

[3] R.K. Rout, A. Kumar, DrP.S. Rao, Encapsulation of oregano (Origanum vulgare) leaf polyphenols: Development, characterization and in-vitro release study, Food Hydrocoll. Health 1 (2021) 100028, https://doi.org/10.1016/j.fhfh.2021.100028.

[4] S.H. Sonawane, B.A. Bhanvase, M. Sivakumar (Eds.), Encapsulation of Active Molecules and Their Delivery System, first ed., Elsevier, Waltham, USA, 2020.

[5] G. Chiarappa, M.D. De'Nobili, A.M. Rojas, M. Abrami, R. Lapasin, G. Grassi, J. A. Ferreira, E. Gudiño, P. de Oliveira, M. Grassi, Mathematical modeling of L-(+)-ascorbic acid delivery from pectin films (packaging) to agar hydrogels (food), J. Food Eng. 234 (2018) 73–81, https://doi.org/10.1016/j.jfoodeng.2018.04.011.

[6] J.D. Oroná, I. Niizawa, B.Y. Espinaco, G.A. Sihufe, S.E. Zorrilla, J.M. Peralta, Mathematical modeling of the release of food active compounds from viscoelastic matrices, J. Food Eng. 288 (2021) 110240, https://doi.org/10.1016/j.jfoodeng.2020.110240.

[7] B.N. Estevinho, F. Rocha, Kinetic models applied to soluble vitamins delivery systems prepared by spray drying, Dry, Technol. 35 (2017) 1249–1257, https://doi.org/10.1080/07373937.2016.1242015.

[8] N. Malekjani, S.M. Jafari, Modeling the release of food bioactive ingredients from carriers/nanocarriers by the empirical, semiempirical, and mechanistic models, Compr. Rev. Food Sci. Food Saf. 20 (2021) 3–47, https://doi.org/10.1111/1541-4337.12660.

[9] J. He, C. Zhong, J. Mi, Modeling of drug release from bioerodible polymer matrices, Drug Deliv. 12 (2005) 251–259, https://doi.org/10.1080/10717540500176043.

[10] R.S. Harland, C. Dubernet, J.-P. Benoît, N.A. Peppas, A model of dissolution-controlled, diffusional drug release from non-swellable polymeric microspheres, J. Contr. Release 7 (1988) 207–215, https://doi.org/10.1016/0168-3659(88)90053-3.

[11] L. Wu, C.S. Brazel, Mathematical model to predict drug release, including the early-time burst effect, from swellable homogeneous hydrogels, Ind. Eng. Chem. Res. 47 (2008) 1518–1526, https://doi.org/10.1021/ie071139m.

[12] J.F. Fitzgerald, O.I. Corrigan, Mechanisms governing drug release from poly-α-hydroxy aliphatic esters: diltiazem base release from poly-lactide-co-glycolide delivery systems, in: M.A. El-Nokaly, D.M. Piatt, B.A. Charpentier (Eds.), Polym. Deliv. Syst., American Chemical Society, 1993, pp. 311–326, https://doi.org/10.1021/bk-1993-0520.ch023. Washington DC, USA.

[13] I. Niizawa, B.Y. Espinaco, S.E. Zorrilla, G.A. Sihufe, Natural astaxanthin encapsulation: use of response surface methodology for the design of alginate

beads, Int. J. Biol. Macromol. 121 (2019) 601–608, https://doi.org/10.1016/j.ijbiomac.2018.10.044.
[14] M.D. De'Nobili, A.M. Rojas, M. Abrami, R. Lapasin, M. Grassi, Structure characterization by means of rheological and NMR experiments as a first necessary approach to study the L-(+)-ascorbic acid diffusion from pectin and pectin/alginate films to agar hydrogels that mimic food materials, J. Food Eng. 165 (2015) 82–92, https://doi.org/10.1016/j.jfoodeng.2015.05.014.
[15] K.J. Karki, S. Samanta, D. Roccatano, Molecular properties of astaxanthin in water/ethanol solutions from computer simulations, J. Phys. Chem. B 120 (2016) 9322–9328, https://doi.org/10.1021/acs.jpcb.6b06055.
[16] J.R. Welty, G.L. Rorrer, D.G. Foster, Fundamentals of Momentum, Heat, and Mass Transfer, sixth ed., John Wiley & Sons, Hoboken, USA, 2015.
[17] Pirayu, Centro de Cómputos del CIMEC, Equipamento en Pirayu. https://cimec.org.ar/c3/pirayu/equipos.php. (Accessed 1 June 2022).
[18] J.J. Montaño Moreno, A. Palmer Pol, A. Sesé Abad, Using the R-MAPE index as a resistant measure of forecast accuracy, Psicothema (2013) 500–506, https://doi.org/10.7334/psicothema2013.23.
[19] E.L. Cussler, Diffusion: Mass Transfer in Fluid Systems, Cambridge University Press, Leiden, 2009. http://public.eblib.com/choice/publicfullrecord.aspx?p=412755.
[20] C. Colín-Chávez, H. Soto-Valdez, E. Peralta, J. Lizardi-Mendoza, R. Balandrán-Quintana, Diffusion of natural astaxanthin from polyethylene active packaging films into a fatty food simulant, Food Res. Int. 54 (2013) 873–880, https://doi.org/10.1016/j.foodres.2013.08.021.
[21] S.K. Bajpai, N. Kirar, Swelling and drug release behavior of calcium alginate/poly (sodium acrylate) hydrogel beads, Des. Monomers Polym. 19 (2016) 89–98, https://doi.org/10.1080/15685551.2015.1092016.
[22] Y.-S. Lin, R.-Y. Tsay, Drug release from a spherical matrix: theoretical analysis for a finite dissolution rate affected by geometric shape of dispersed drugs, Pharmaceutics 12 (2020) 582, https://doi.org/10.3390/pharmaceutics12060582.
[23] B.T. Smith, Solubility and dissolution, in: Phys. Pharm., first ed., Pharmaceuthical Press, 2015.
[24] G.-P. Yan, H. Li, S.-X. Cheng, S.E. Bottle, X.-G. Wang, Y.K. Yew, R.-X. Zhuo, Preparation, properties, and mathematical modeling of microparticle drug delivery systems based on biodegradable amphiphilic triblock copolymers, J. Appl. Polym. Sci. 92 (2004) 3869–3873, https://doi.org/10.1002/app.20410.
[25] F. Mohr, R. Steffen, Physiology of gastrointestinal motility, in: R. Wyllie, J. S. Hyams (Eds.), Pediatr. Gastrointest. Liver Dis., fourth ed., Elsevier Saunders, Philadelphia, USA, 2011, pp. 39–49, https://doi.org/10.1016/B978-1-4377-0774-8.10005-3.
[26] M. Ahearne, Y. Yang, A.J. El Haj, K.Y. Then, K.-K. Liu, Characterizing the viscoelastic properties of thin hydrogel-based constructs for tissue engineering applications, J. R. Soc. Interface 2 (2005) 455–463, https://doi.org/10.1098/rsif.2005.0065.
[27] M. Grassi, R. Lapasin, S. Pricl, Modeling of drug release from a swellable matrix, Chem. Eng. Commun. 169 (1998) 79–109, https://doi.org/10.1080/00986449808912722.
[28] D. Caccavo, An overview on the mathematical modeling of hydrogels' behavior for drug delivery systems, Int. J. Pharm. 560 (2019) 175–190, https://doi.org/10.1016/j.ijpharm.2019.01.076.
[29] M. Llorens-Gámez, Á. Serrano-Aroca, Low-cost advanced hydrogels of calcium alginate/carbon nanofibers with enhanced water diffusion and compression properties, Polymers 10 (2018) 405, https://doi.org/10.3390/polym10040405.
[30] M. Holz, S.R. Heil, A. Sacco, Temperature-dependent self-diffusion coefficients of water and six selected molecular liquids for calibration in accurate 1H NMR PFG measurements, Phys. Chem. Chem. Phys. 2 (2000) 4740–4742, https://doi.org/10.1039/b005319h.